

THÈSE

Pour obtenir le grade de

DOCTEUR DE L'UNIVERSITÉ DE GRENOBLE

Spécialité : **Informatique**

Arrêté ministériel : 25 mai 2016

Présentée par

Tom CORNEBIZE

Thèse dirigée par **Arnaud LEGRAND**

préparée au sein du **Laboratoire d'Informatique de Grenoble**
et de l'École Doctorale **MSTII**

Le Titre de la Thèse

The English Title

Thèse soutenue publiquement le **1^{er} janvier 1970**,
devant le jury composé de :



I dedicate this thesis to my grumpy cat.

DRAFT

4th November 2020, 13:41:54

” *Elle est où la poulette ?*

— **Kadoc DE VANNES**

DRAFT

4th November 2020, 13:41:54

Remerciements

(Acknowledgments)

I would like to thank everyone, except from Dobby the free elf.

Merci public !

DRAFT

4th November 2020, 13:41:54

Abstract / Résumé

Abstract

The English abstract.

DRAFT

4th November 2020, 13:41:54

Résumé

Le résumé en français.

DRAFT

4th November 2020, 13:41:54

Contents

Acknowledgments	v
Abstract / Résumé	vii
Contents	ix
Introduction	1
I. Performance prediction through simulation: the HPL case	3
1. High Performance Linpack	7
1.1. The benchmark	7
1.2. Typical runs on a supercomputer	9
2. Related work	11
2.1. Performance prediction	11
2.2. Simgrid/SMPI	12
3. Emulating HPL at large scale	15
3.1. Speeding Up the Emulation	15
3.1.1. Compute Kernel Modeling	15
3.1.2. Specific Adjustments	16
3.2. Scaling Down Memory Consumption	17
3.3. Scalability Evaluation	19
4. Modeling HPL kernels and communications	21
4.1. Modeling notations	21
4.2. Modeling the CPU (i.e. dgemm function)	23
4.2.1. Different linear models	23
4.2.2. Bayesian modeling and generative models	25
4.2.3. Conclusion	25
4.3. Modeling the network	25
4.3.1. Modelisation in Simgrid	25
4.3.2. Learning breakpoints	26

4.4. Conclusion	26
5. Validation	27
5.1. Different problem sizes	27
5.2. A platform change	27
5.3. Factorial experiment	27
5.4. Different geometries	27
5.5. Conclusion	27
6. Sensibility analysis	29
6.1. Influence of temporal variability	29
6.2. Influence of spatial variability	29
6.3. Influence of the physical topology	29
II. Experimental control	31
7. Experimental Testbed and Experiment Engines	33
7.1. State of the art	33
7.1.1. Grid'5000	33
7.1.2. Experiment engines	33
7.2. Yet another experiment engine: Peanut	34
7.2.1. Key features	34
7.2.2. Comparison with Execo	34
8. Randomizing matters!	35
8.1. Basic effects	35
8.2. Unexpected effects	35
8.3. Beware of extrapolations	35
8.4. Beware of experimental conditions	35
8.5. Conclusion	35
9. Performance non-regression tests	37
9.1. State of the art	37
9.2. Performance measure and information collection	37
9.3. Statistical test	37
9.4. Conclusion	37
Conclusion	39
Bibliography	A1

List of Figures

A5

List of Tables

A5

DRAFT

4th November 2020, 13:41:54

Introduction

To introduce my work, I will write a nice introduction in the following. Citation example for the Top500 website [@top500] and some random paper [Gra69].

Lorem ipsum dolor sit amet, consectetur adipiscing elit. Ut purus elit, vestibulum ut, placerat ac, adipiscing vitae, felis. Curabitur dictum gravida mauris. Nam arcu libero, nonummy eget, consectetur id, vulputate a, magna. Donec vehicula augue eu neque. Pellentesque habitant morbi tristique senectus et netus et malesuada fames ac turpis egestas. Mauris ut leo. Cras viverra metus rhoncus sem. Nulla et lectus vestibulum urna fringilla ultrices. Phasellus eu tellus sit amet tortor gravida placerat. Integer sapien est, iaculis in, pretium quis, viverra ac, nunc. Praesent eget sem vel leo ultrices bibendum. Aenean faucibus. Morbi dolor nulla, malesuada eu, pulvinar at, mollis ac, nulla. Curabitur auctor semper nulla. Donec varius orci eget risus. Duis nibh mi, congue eu, accumsan eleifend, sagittis quis, diam. Duis eget orci sit amet orci dignissim rutrum.

4th November 2020, 13:41:54

Part I

Performance prediction through simulation:
the HPL case

DRAFT

4th November 2020, 13:41:54

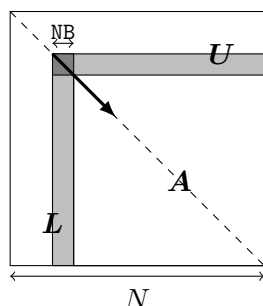
The work presented in this part has been published at a conference[CLH19] and has been submitted for publication in a journal. The content of this part is therefore a near-verbatim copy of these articles. This work also directly follows my master thesis[Cor17] whose main contribution is summarized in chapter 3 for the sake of completeness.

DRAFT

4th November 2020, 13:41:54

High Performance Linpack

1.1 The benchmark



```

allocate and initialize A;
for  $k = N$  to 0 step  $NB$  do
    allocate the panel;
    factor the panel;
    broadcast the panel;
    update the sub-matrix;
end

```

Figure 1.1.: Overview of High Performance Linpack

In this work, we use the freely-available reference-implementation of HPL[Pet+16], which relies on MPI. HPL implements a matrix factorization based on a right-looking variant of the LU factorization with row partial pivoting and allows multiple look-ahead depths. The principle of the factorization is depicted in Figure 1.1. It consists of a series of panel factorizations followed by an update of the trailing sub-matrix. HPL uses a two-dimensional block-cyclic data distribution of A and implements several custom MPI collective communication algorithms to efficiently overlap communications with computations. The main parameters of HPL are:

- N is the order of the square matrix A .
- NB is the *blocking factor*, i.e. the granularity at which HPL operates when panels are distributed or worked on.
- P and Q denote the number of process rows and the number of process columns, respectively.
- $RFACT$ determines the panel factorization algorithm. Possible values are Crout, left- or right-looking.
- $SWAP$ specifies the swapping algorithm used while pivoting. Two algorithms are available: one based on *binary exchange* (along a virtual tree topology) and the other one based on a *spread-and-roll* (with a higher number of parallel

communications). HPL also provides a panel-size threshold triggering a switch from one variant to the other.

- **BCAST** sets the algorithm used to broadcast a panel of columns over the process columns. Legacy versions of the MPI standard only supported non-blocking point-to-point communications, which is why HPL ships with in total 6 self-implemented variants to overlap the time spent waiting for an incoming panel with updates to the trailing matrix: `ring`, `ring-modified`, `2-ring`, `2-ring-modified`, `long`, and `long-modified`. The modified versions guarantee that the process right after the root (i.e. the process that will become the root in the next iteration) receives data first and does not further participate in the broadcast. This process can thereby start working on the panel as soon as possible. The `ring` and `2-ring` versions each broadcast along the corresponding virtual topologies while the `long` version is a *spread and roll* algorithm where messages are chopped into Q pieces. This generally leads to better bandwidth exploitation. The `ring` and `2-ring` variants rely on `MPI_Iprobe`, meaning they return control if no message has been fully received yet, hence facilitating partial overlap of communication with computations. In HPL 2.1 and 2.2, this capability has been deactivated for the `long` and `long-modified` algorithms. A comment in the source code states that some machines apparently get stuck when there are too many ongoing messages.
- **DEPTH** controls how many iterations of the outer loop can overlap with each other.

The sequential complexity of this factorization is

$$\text{flop}(N) = \frac{2}{3}N^3 + 2N^2 + \mathcal{O}(N)$$

where N is the order of the matrix to factorize. The time complexity can be approximated by

$$T(N) \approx \frac{\left(\frac{2}{3}N^3 + 2N^2\right)}{P \cdot Q \cdot w} + \Theta((P + Q) \cdot N^2)$$

where w is the flop rate of a single node and the second term corresponds to the communication overhead which is influenced by the network capacity and the previously listed parameters (`RFACT`, `SWAP`, `BCAST`, `DEPTH`, ...) and is very difficult to predict.

1.2 Typical runs on a supercomputer

Although the TOP500 reports precise information about the core count, the peak performance and the effective performance, it provides almost no information on how (software versions, HPL parameters, etc.) this performance was achieved. Some colleagues agreed to provide us with the HPL configuration they used and the output they submitted for ranking (see Table 1.1). In June 2013, the Stampede supercomputer at TACC was ranked 6th in the TOP500 by achieving $5168.1 \text{ TFlop s}^{-1}$. In November 2017, the Theta supercomputer at ANL was ranked 18th with a performance of $5884.6 \text{ TFlop s}^{-1}$ but required a 28-hour run on the whole machine. Finally, we ran HPL ourselves on a Grid'5000 cluster named Dahu whose software stack could be fully controlled.

Table 1.1.: Typical runs of HPL

	Stampede@TACC	Theta@ANL	Dahu@G5K
Rpeak	$8520.1 \text{ TFlop s}^{-1}$	$9627.2 \text{ TFlop s}^{-1}$	$62.26 \text{ TFlop s}^{-1}$
N	3,875,000	8,360,352	500,000
NB	1024	336	128
$P \times Q$	77×78	32×101	32×32
RFACT	Crout	Left	Right
SWAP	Binary-exch.	Binary-exch.	Binary-exch.
BCAST	Long modified	2 Ring modified	2 Ring
DEPTH	0	0	1
Rmax	$5168.1 \text{ TFlop s}^{-1}$	$5884.6 \text{ TFlop s}^{-1}$	$24.55 \text{ TFlop s}^{-1}$
Duration	2 hours	28 hours	1 hour
Memory	120 TB	559 TB	2 TB
MPI ranks	1/node	1/node	1/core

The performance typically achieved by supercomputers (Rmax) needs to be compared to the much larger peak performance (Rpeak). This difference can be attributed to the node usage, to the MPI library, to the network topology that may be unable to deal with the intense communication workload, to load imbalance among nodes (e.g. due to a defect, system noise, ...), to the algorithmic structure of HPL, etc. All these factors make it difficult to know precisely what performance to expect without running the application at scale. It is clear that due to the level of complexity of both HPL and the underlying hardware, simple performance models (analytic expressions based on N, P, Q and estimations of platform characteristics) may be able to provide trends but can by no means accurately predict the performance for each configuration (e.g. consider the exact effect of HPL's six different broadcast algorithms on network contention). Additionally, these expressions do not allow engineers to improve the performance through actively identifying performance bottlenecks. For complex optimizations such as partially non-blocking collective

communication algorithms intertwined with computations, a very faithful modeling of both the application and the platform is required. One goal of this thesis was to simulate systems at the scale of Stampede. Given the scale of this scenario (3,785 steps on 6,006 nodes in two hours), detailed simulations quickly become intractable without significant effort.

DRAFT

4th November 2020, 13:41:54

Related work

2.1 Performance prediction

A first approach for estimating the performance of applications like HPL is statistical modeling of the application as a whole[LD12]. By running the application several times with small and medium problem sizes (of a few iterations of large problem sizes) and using simple linear regressions, it is possible to predict its makespan for larger sizes with an error of only a few percents and a relatively low cost. Unfortunately, the predictions are limited to the same application configuration and studying the influence of the number of rows and columns of the virtual grid or of the broadcast algorithms requires a new model and new (costly) runs using the whole target machine. Furthermore, this approach does not allow to study what-if scenarios (e.g. to evaluate what would happen if the network bandwidth was increased or if node heterogeneity was decreased) that are particularly useful when investigating potential performance improvements.

Simulation provides the details and flexibility missing to such black-box modeling approach. Performance prediction of MPI applications through simulation has been widely studied over the last decades but two approaches can be distinguished in the literature: offline and online simulation.

With the most common approach, *offline simulation*, a trace of the application is first obtained on a real platform. This trace comprises sequences of MPI operations and CPU bursts and is given as an input to a simulator that implements performance models for the CPUs and the network to derive predictions. Researchers interested in finding out how their application reacts to changes to the underlying platform can replay the trace on commodity hardware at will with different platform models. Most HPC simulators available today, notably BigSim[ZKK04], Dimemas[Bad+03] and CODES[Mub+16], rely on this approach. The main limitation of this approach comes from the trace acquisition requirement. Not only is a large machine required but the compressed trace of a few iterations (out of several thousands) of HPL typically reaches a few hundred MB, making this approach quickly impractical[Cas+15]. Worse, tracing an application provides only information about its behavior at the time of the run: slight modifications (e.g. to communication patterns) may make

the trace inaccurate. The behavior of simple applications (e.g. `stencil`) can be extrapolated from small-scale traces[WM11; CLT13] but this fails if the execution is non-deterministic, e.g. whenever the application relies on non-blocking communication patterns, which is unfortunately the case for HPL.

The second approach discussed in the literature is *online simulation*. Here, the application is executed (emulated) on top of a simulator that is responsible to determine when each process is run. This approach allows researchers to study directly the behavior of MPI applications but only a few recent simulators such as SST Macro[Jan+10], SimGrid/SMPI[Cas+14] and the closed-source xSim[Eng14] support it. To the best of our knowledge, only SST Macro and SimGrid/SMPI are mature enough to faithfully emulate HPL. This work relies on SimGrid as its performance models and its emulation capabilities seemed quite solid but the proposed developments would a priori also be possible with SST. Note that the HPL emulation described in chapter 3 should not be confused with the application skeletonization[Bir+13] commonly used with SST. Skeletons are code extractions of the most important parts of a complex application whereas we only modify a few dozens of lines of HPL before emulating it with SMPI. Finally, it is important to understand that the proposed approach is intended to help studies at the level of the whole machine and application, not the influence of microarchitectural details as intended by MUSA[Gra+16].

2.2 Simgrid/SMPI

SimGrid[Cas+14] is a flexible and open-source simulation framework that was originally designed in 2000 to study scheduling heuristics tailored to heterogeneous grid computing environments but has later been extended to study cloud and HPC infrastructures. The main development goal for SimGrid has been to provide validated performance models particularly for scenarios making heavy use of the network. Such a validation usually consists of comparing simulation predictions with results from real experiments to confirm or debunk network and application models.

SMPI, a simulator based on SimGrid, has been developed and used to simulate unmodified MPI applications written in C/C++ or FORTRAN[Deg+17]. The complex network optimizations done in real MPI implementations need to be considered when predicting the performance of MPI applications. For instance, the "eager" and "rendez-vous" protocols are selected based on the message size, with each

protocol having its own synchronization semantics, which strongly impact performance. SMPI supports different performance modes through a generalization of the LogGPS model. Another difficult issue is to model network topologies and contention. SMPI relies on SimGrid's communication models where each ongoing communication is represented as a whole (as opposed to single packets) by a *flow*. Assuming steady-state, contention between active communications can then be modeled as a bandwidth sharing problem that accounts for non-trivial phenomena (e.g. cross-traffic interference[Vel+13]). If needed, communications that start or end trigger a re-computation of the bandwidth share. In this fluid model, the time to simulate a message passing through the network is independent of its size, which is advantageous for large-scale applications frequently sending large messages and orders of magnitude faster than packet-level simulation. SimGrid does not model transient phenomena incurred by the network protocol but accounts for network topology and heterogeneity. Special attention to the modeling of collective communication algorithms has also been paid in SMPI, but this is of little significance in this article as HPL ships with its own implementation of collective operations.

SMPI maps every MPI rank of the application onto a lightweight simulation thread. These threads are then run one at a time, i.e. in mutual exclusion. Every time a thread enters an MPI call, SMPI takes control and the time that was spent computing (isolated from the other threads) since the previous MPI call is injected into the simulator as a virtual delay. This time may be scaled up or down depending on the speed of the simulated machine with respect to the simulation machine. Recent results report consistent performance predictions within a few percent for standard benchmarks on small-scale clusters (up to 12×12 cores [Hei+17] and up to 128×1 cores [Deg+17]). In this thesis, I validate this approach at a much larger scale with HPL, whose emulation comes with at least two challenges:

- The time-complexity of the algorithm is $\Theta(N^3)$ and $\Theta(N^2)$ communications are performed, with N being very large. The execution on the Stampede cluster took roughly two hours on 6006 compute nodes. Using only a single node, a naive emulation of HPL at the scale of the Stampede run would take about 500 days if perfect scaling was reached.
- The tremendous memory consumption and amount of memory accesses need to be drastically reduced.

Emulating HPL at large scale

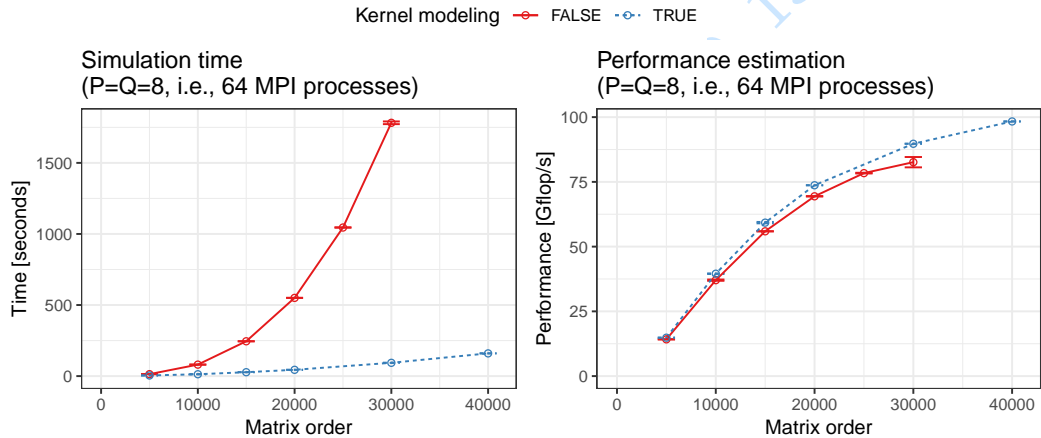
In this chapter, we present the changes to SimGrid and HPL that were required for a scalable simulation. The experiments were done using a single core from nodes of the Nova cluster provided by the Grid'5000 testbed[Bal+13] (32 GB of RAM, two 8-core Intel Xeon E5-2620 v4 CPUs, Debian Stretch OS (Linux 4.9)).

3.1 Speeding Up the Emulation

3.1.1 Compute Kernel Modeling

```
#define HPL_dgemm(layout, TransA, TransB, M, N, K,      \
    alpha, A, lda, B, ldb, beta, C, ldc) ({           \
    double size = ((double)M)*((double)N)*((double)K); \
    double expected_time = 1.029e-11*size + 1.981e-12; \
    smpi_execute_benchded(expected_time);              \
})
```

(a) Non-intrusive macro replacement with a very simple computation model.



(b) Gain in terms of simulation time.

Figure 3.1.: Replacing the calls to computationally expensive functions by a model allows to emulate HPL at a larger scale.

HPL heavily relies on BLAS kernels such as `dgemm` (for matrix-matrix multiplication) or `dtrsm` (for solving an $A \cdot x = b$ equation). The analysis of an HPL simulation

with 64 processes and a very small matrix of order 30,000 showed that about 96 % of the time is spent in these two kernels. Since the output of these kernels does not influence the control flow, simulation time can be reduced by substituting `dgemm` and `dtrsm` function calls with a performance model of the respective kernel. Skipping kernels renders the content of some variables invalid but in simulation, only the behavior of the application and not the correctness of computation results are of concern. Figure 3.1(a) shows an example of this macro-based mechanism that allows to keep HPL code modifications to an absolute minimum. The $(1.029e-11)$ value represents the inverse of the flop rate for this compute kernel and was obtained through calibration. The estimated time of the kernel is calculated based on the given parameters and passed on to `smpi_execute_bench` that advances the clock of the executing rank by this estimate. The effect on the simulation time for a small scenario is depicted in Figure 3.1(b). This modification speeds up the simulation by orders of magnitude. The precision of the simulation will be investigated in more details in the next chapter but it can already be observed that this simple kernel model leads to a sound, albeit slightly more optimistic, estimation of the performance.

In addition to the main compute kernels, a profiling of the code allowed to identify seven other BLAS functions as computationally expensive enough to justify a specific handling: `dgemv`, `dswap`, `daxpy`, `dscal`, `dtrsv`, `dger` and `idamax`. Similarly, a significant amount of time was spent in fifteen functions implemented in HPL: `HPL_dlaswp*N`, `HPL_dlaswp*T`, `HPL_dlacpy` and `HPL_dlatcpy`. All these functions are called during the LU factorization and hence impact the performance measured by HPL; however, because of the removal of the `dgemm` and `dtrsm` computations, they all operate on bogus data and hence also produce bogus data. They have been handled similarly to `dgemm` and `dtrsm`, through performance models and macro substitution, which speeds up the simulation by an additional factor of 3 to 4 on small ($N = 30,000$) and even more on large scenarios.

3.1.2 Specific Adjustments

HPL uses pseudo-randomly generated matrices that are setup every time HPL is executed. This initialization, just like the factorization correctness verification at the end of the run, is not considered in the reported performance and can therefore be safely skipped. Note that HPL implements an LU factorization with partial pivoting, which requires a special treatment of the `idamax` function that returns the index of the first element equaling the maximum absolute value. Although the cost of this

function was ignored as well, its return value was has been set to a random (but controlled) value to make the simulation unbiased (but fully deterministic).

3.2 Scaling Down Memory Consumption

The largest two allocated data structures in HPL are the input matrix *A* (with a size of typically several GB per process) and the *panel* which contains information about the sub-matrix currently being factorized. This sub-matrix typically occupies a few hundred MB per process. Unfortunately, when emulating an application with SMPI, all MPI processes are run within the same simulation process on a single node and the memory consumption of the simulation can therefore quickly reach several TB of RAM. Yet, as we no longer operate on real data, storing the whole input matrix *A* is needless. However, since only a minimal portion of the code was modified, some functions may still read or write some parts of the matrix. It is thus not possible to simply remove the memory allocations of large data structures. SMPI provides the `SMPI_SHARED_MALLOC` (`SMPI_SHARED_FREE`) macro to replace calls to `malloc` (`free`). They indicate that some data structures can safely be shared between processes and that the data they contain is not critical for the execution (e.g. an input matrix) and that it may even be overwritten. `SMPI_SHARED_MALLOC` works as follows (see Figure3.2): a single block of physical memory (of default size 1 MB) for the whole execution is allocated and shared by all MPI processes. A range of virtual addresses corresponding to a specified size is reserved and cyclically mapped onto the previously obtained physical address. This mechanism allows most applications to obtain a nearly constant memory footprint, regardless of the size of the actual allocations.

Although using the default `SHARED_MALLOC` mechanism works flawlessly for *A*, a more careful strategy needs to be used for the *panel*, which is an intricate data structure with both `ints` (accounting for matrix indices, error codes, MPI tags, and pivoting information) and `doubles` (corresponding to a copy of a sub-matrix of *A*). To optimize data transfers, HPL flattens this structure into a single allocation of `doubles` (see Figure3.3(a)). Using a fully shared memory allocation for the *panel* therefore leads to index corruption that results in classic invalid memory accesses. Since `ints` and `doubles` are stored in non-contiguous parts of this flat allocation, it is therefore essential to have a mechanism that preserves the process-specific content. We have thus introduced the `SMPI_PARTIAL_SHARED_MALLOC` macro that allows us to specify which ranges of the allocation should be preserved (i.e. are private to each process) and which ones may be corrupted (i.e. are shared between processes).

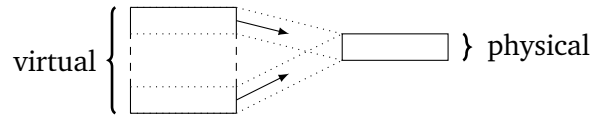
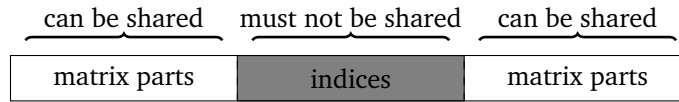
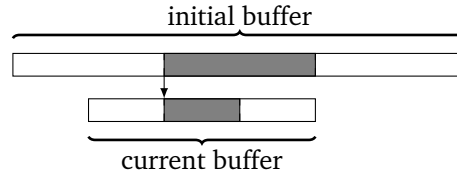


Figure 3.2.: SMPI shared malloc mechanism: large area of virtual memory are mapped onto the same physical pages.



(a) Structure of the panel in HPL.



(b) Reusing panel allocation from an iteration to another.

Figure 3.3.: Panel structure and allocation strategy.

For a matrix of order 40,000 and 64 MPI processes, memory consumption decreases with this approach from about 13.5 GB to less than 40 MB.

Another HPL specific optimization is related to the systematic allocation and deallocation of panels in each iteration, with the size of the panel strictly decreasing from iteration to iteration. As explained above, the partial sharing of panels requires many calls to `mmap` and introduces an overhead that makes these repeated allocations / frees a bottleneck. Since the very first allocation can fit all subsequent panels, we modified this allocation mechanism so that SMPI can reuse panels as much as possible from an iteration to an other (see Figure 3.3(b)). Even for a very small matrix of order 40,000 and 64 MPI processes, the simulation time decreases from 20.5 sec to 16.5 sec. The number of page faults decreased from 2 million to 0.2 million, confirming the devastating effect these allocations/deallocations would have at scale.

The next three optimizations are not specific to HPL. We leveraged the information on which memory area is private, shared or partially shared to improve the overall performance. By making SMPI internally aware of the memory's visibility, it can now avoid calling `memcpy` when large messages containing shared segments are sent from one MPI rank to another. For fully private or partially shared segments, SMPI identifies and copies only those parts that are process-dependent (private) into the corresponding buffers on the receiver side. HPL simulation times and memory consumption were considerably improved in our experiments because the panel is

the most frequently transferred data structure but only a small part of it is actually private.

As explained above, SMPI maps MPI processes to threads of a single process, effectively folding them into the same address space. Consequently, global variables in the MPI application are shared between threads unless these variables are *privatized* and the simulated MPI ranks thus isolated from each other. Several technical solutions are possible to handle this issue [Deg+17]. The default strategy in SMPI consists in making a copy of the data segment (containing all global variables) per MPI rank at startup and, when context switching to another rank, to remap the data segment via `mmap` to the private copy of that rank. SMPI also implements another mechanism relying on the `dlopen` function that allows to load several times the data segment in memory and to avoid costly calls to `mmap` (and subsequent cache flush) when context switching. For a matrix of order 80,000 and 32 MPI processes, the number of minor page faults drops from 4,412,047 (with `mmap`) to 6880 (with `dlopen`), which results in a reduction of system time from 10.64 sec (out of 51.47 sec) to 2.12 sec.

Finally, for larger matrix orders (i.e. N larger than a few hundred thousands), the performance of the simulation quickly deteriorates as the memory consumption rises rapidly. Indeed, folding the memory reduces the *physical* memory usage. The *virtual* memory, on the other hand, is still allocated for every process since the allocation calls are still executed. Without a reduction of allocated virtual addresses, the page table rapidly becomes too large for a single node. Thankfully, the x86-64 architecture supports several page sizes, such as the *huge pages* in Linux. Typically, these pages are around 2 MiB (instead of 4 KiB), which reduces drastically the page table size. For example, for a matrix of order $N = 4,000,000$, it shrinks from 250 GB to 0.488 GB.

3.3 Scalability Evaluation

The main goal of the previous optimizations is to reduce the complexity from $\Theta(N^3) + \Theta(N^2 \cdot P \cdot Q)$ to something more reasonable. The $\Theta(N^3)$ was removed by skipping most computations. Ideally, since there are N/NB iterations (steps), the complexity of simulating one step should be decreased to something independent of N . SimGrid's fluid models, used to simulate communications, do not depend on N . Therefore, the time to simulate a step of HPL should mostly depend on P and Q . Yet, some memory operations on the panel that are related to pivoting are intertwined



Figure 3.4.: Time complexity and memory consumption are linear in the number of processes but remain mildly quadratic with matrix rank.

in HPL with collective communications, meaning that it is impossible to get rid of the $\mathcal{O}(N)$ complexity without modifying HPL more profoundly.

To evaluate the efficiency of our proposal, we conduct a first evaluation on a non-existing but Stampede resembling platform comprising 4,096 nodes interconnected through a fat-tree topology. We run simulations with 512, 1024, 2048 or 4096 MPI ranks and with matrices of orders 5×10^5 , 1×10^6 , 2×10^6 or 4×10^6 . All other HPL parameters are similar to the ones of the original Stampede scenario. The impact of the matrix order on total makespan and memory is illustrated in Figure 3.4. With all previously described optimizations enabled, the longest simulation took close to 47 hours and consumed 16 GB of memory whereas the shortest one took 20 minutes and 282 MB of memory.

Modeling HPL kernels and communications

As explained in chapter 3, HPL spends most of its computation time in a dozen specific functions for which a performance model has to be designed. Most compute kernels have several parameters from which a very simple model can generally easily be identified (e.g. proportional to the product of the parameters) but refinements including the individual contribution of each parameter as well as the spatial and temporal variability of the operation are also possible. Likewise, communications between two nodes are mostly linear in message size but the actual performance can wildly vary depending on the range of the message size as MPI switches from one protocol to another whenever needed. In this chapter we first introduce some notations to describe the complexity of the models we have investigated. We then briefly compare the prediction of these models with individual measurements of both computations and communications to illustrate the importance of the model complexity.

4.1 Modeling notations

We denote as T the duration of an operation with parameters M, N, K (in the case of the `dgemm` operation, these parameters describe the geometry of the input matrices). We first consider the three following modeling options:

- Modeling option $\mathcal{M}-0$: For simple and stable compute kernels, the duration can be modeled as a constant duration independent of the input parameters, i.e. $T \sim \alpha$, where α is estimated through the sample average of the duration of the operation (or simply 0 if the kernel is negligible) .
- Modeling option $\mathcal{M}-1$: A simple combination of the parameters (e.g. $S = M.N.K$) may be the primary factor driving the performance of the operation. Then $T \sim \alpha.S (+\beta)$ and α and β can be estimated through a classical least-square linear regression.

- Modeling option $\mathcal{M}-2$: When the behavior of the operation is complex or requires a faithful modeling over the full range of input parameters, a full polynomial model is required, i.e. $T \sim \alpha.M.N.K + \beta.M.N + \gamma.N.P + \dots$. Again, the $\alpha, \beta, \gamma, \dots$ can be estimated through a classical least-square linear regression.

There are two situations where more elaborate variations need to be considered:

- Whenever the platform is slightly heterogeneous (spatial variability), the previous models should be built for each host individually. This modeling option is denoted \mathcal{M}_H .
- The behavior of the operation may be mostly linear but only for specific parameter ranges. This is for example the case for networking operations or for computing nodes on Stampede where Intel's Math Kernel Library (MKL) uses the Xeon Phi accelerator only when the input is large enough to compensate for the data transfer. In such situations, the models considered will be piece-wise linear,

$$\text{e.g., } T \sim \begin{cases} \text{if } M < \theta_1 & \alpha_1.M + \beta_1 \\ \text{else if } M < \theta_2 & \alpha_2.M + \beta_2, \\ \dots \end{cases}$$

where the θ, α, β should all be estimated. This kind of model is denoted \mathcal{M}' .

All previous models can be fit with relatively simple linear regressions or maximum likelihood learning methods. However, an important hypothesis underlying all these methods is the homoscedasticity, i.e. that the variability is independent on the parameters.

The residual (temporal) variability may be an important phenomenon to account for, as "system noise" is known to be detrimental to the overall performance of parallel applications like HPL. We thus consider different modeling options for this temporal variability:

- Noise option $\mathcal{N}-0$ (no noise): This is the simplest option. It consists in injecting the value predicted by the model
- Noise option $\mathcal{N}-1$ (homoscedastic): The simplest probability family to model variability is the normal distribution, hence $T \sim \mathcal{M}(M, N, K) + N(0, \sigma^2)$, where σ^2 is the sample variance of the model residuals.

- Noise option $\mathcal{N}-2$ (heteroscedastic): The conditional variance of the residuals (i.e. σ^2 given M, N, K) is modeled by a polynomial function of the input parameters.

Finally, even the sophisticated normal distribution from $\mathcal{N}-2$ may be too simple to describe the noise observed on real platforms where it may be common for a same parameter set to have a few operations being one order of magnitude slower than all the other ones. In this case, a reasonable option consists of modeling noise with a mixture of normal distributions whose parameters π_1, \dots, π_k should be estimated. We denote this kind of model as \mathcal{N}' . Likewise, the per-host estimations are denoted by \mathcal{N}_H .

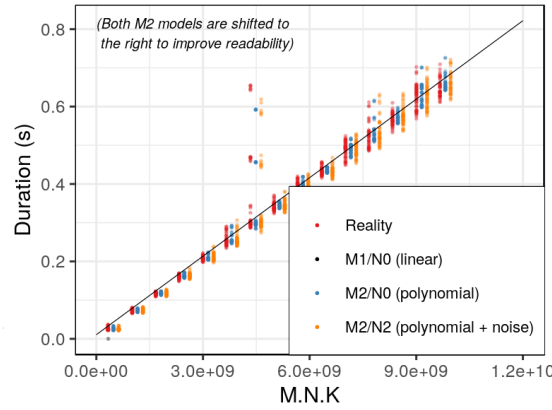
4.2 Modeling the CPU (i.e. dgemm function)

4.2.1 Different linear models

HPL spends the most time in the dgemm kernel, it is therefore of extreme importance to model this function very faithfully. We evaluated the previous modeling alternatives: $\mathcal{M}-\{1, 2\}$, $\mathcal{N}-\{0, 1, 2\}$ and $\mathcal{M}_H-\{1, 2\}$, $\mathcal{N}_H-\{0, 1, 2\}$. The \mathcal{M}' and \mathcal{N}' families were not investigated as nothing in our observations called for such complexity on classical multi-core machines. Figure 4.1 illustrates various models and their respective quality for the dgemm function. In these figures, the performance of dgemm is evaluated by calling dgemm with randomized sizes over all the cores of each node (to reproduce experimental conditions similar to the one of HPL). The first observation (Figure 4.1(a)) is that a few nodes exhibit quite a different behavior (each color and each regression line under model \mathcal{M}_H-1 corresponds to a different cpu, whereas the black dotted line corresponds to model $\mathcal{M}-1$ over all the nodes). These nodes will systematically be slightly slower than other nodes and accounting for this spatial heterogeneity is likely to be rather important for HPL. Second, we took care of covering a wide variety of combinations for M , N , and K and it can be observed that $M.N.K$ is not sufficient to describe correctly the performance of dgemm. Indeed, for $M.N.K \approx 4.5 \times 10^9$ some duration are systematically higher regardless of the node. This happens for some particular (e.g., tall and skinny) matrix geometries, which strongly suggests using the full polynomial model. Figure 4.1(b) depicts the performance (red dots) of a given node as well as the prediction using a simple linear model (\mathcal{M}_H-1 , black line), a full polynomial model (\mathcal{M}_H-2 , blue dots) and a full polynomial model with heteroscedastic noise (\mathcal{M}_H-2 \mathcal{N}_H-2 , orange dots). A close inspection reveals that all experimental variability is actually very



(a) dgemm heterogeneity



(b) dgemm model

Figure 4.1.: Illustrating the realism of modeling for dgemm function

well explained by both the polynomial model (better fit for particular parameter combinations) and some temporal variability.

Four other BLAS kernels and a few other very small HPL compute kernels (often related to memory management) are deeply intertwined with collective operations to allow HPL to be as efficient as possible. Although the total duration of these kernels is extremely small compared to the total execution time, they may perturb collective communication by introducing late sends and receives. The behavior of one of these kernels is illustrated in Figure 4.2. This kind of data can only be obtained by running HPL for a small input matrix over each node individually. Again, for all these kernels a single parameter combination explains most of the performance and there is some variability from one node to another (one blue regression line per CPU) but it remains quite limited (black dotted line for the platform as a whole), especially since these kernels are very short and infrequently called compared to



Figure 4.2.: Illustrating the realism of modeling for HPL_dlatcpy function

dgemm. Finally, since variability significantly increases with the value of the input parameters, a $\mathcal{N}-2$ model is clearly required. The blue dots in Figure 4.2 represent the outcome of a $\mathcal{M}-1 \mathcal{N}-2$ model and are hardly distinguishable from the real behavior. Similar results can be obtained with this category of model for all other kernels.

4.2.2 Bayesian modeling and generative models

Some text...

4.2.3 Conclusion

Some text...

4.3 Modeling the network

4.3.1 Modelisation in Simgrid

Prior to this work, the standard way of accounting for protocol changes in SMPI was to estimate breakpoints visually and to conduct a linear regression for each range. The expected duration was then used directly in the simulation with no particular effort with respect to the temporal variability ($\mathcal{M}'-1 \mathcal{N}-0$). Yet, as illustrated in Figure 4.3, the variability of high speed networks is quite particular. We therefore

diligently estimated all the parameters of $\mathcal{M}' - 1 \mathcal{N}' - 1$, where each message size range is automatically estimated with `pytree`, as well as the 2 to 4 modes of the Gaussian mixture for each range. Such temporal variability could explain some (overall bad) performance since they generally get amplified by broadcast and pipelined communication patterns.

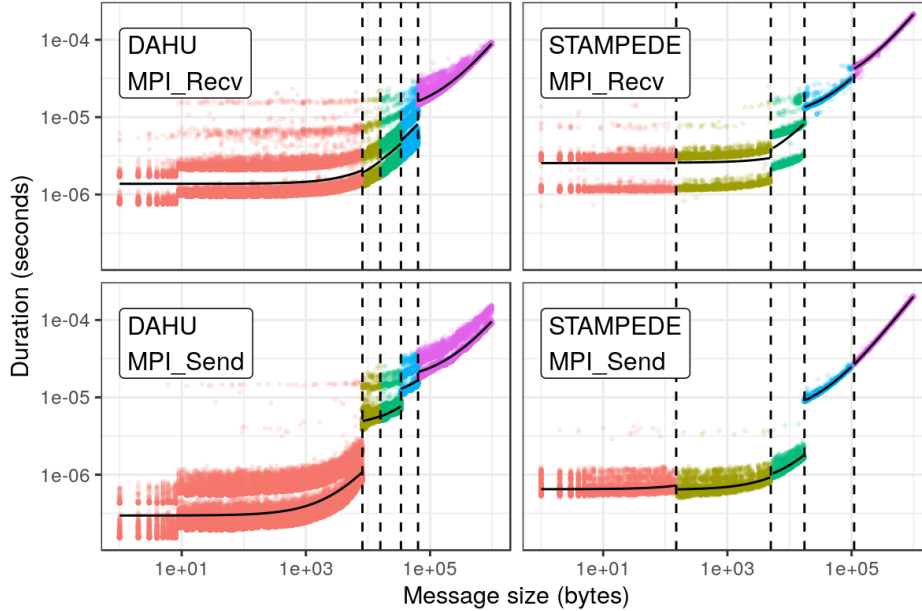


Figure 4.3.: Illustrating piecewise linearity and temporal variability of high-speed communications on two systems.

4.3.2 Learning breakpoints

Some text. . .

4.4 Conclusion

Some text. . .

Validation

5.1 Different problem sizes

Some text. . .

5.2 A platform change

Some text. . .

5.3 Factorial experiment

Some text. . .

5.4 Different geometries

Some text. . .

5.5 Conclusion

DRAFT
4th November 2020, 13:41:54

Sensibility analysis

6.1 Influence of temporal variability

Some text...

6.2 Influence of spatial variability

Some text...

6.3 Influence of the physical topology

Some text...

DRAFT
4th November 2020, 13:41:54

Part II

Experimental control

DRAFT

4th November 2020, 13:41:51

Experimental Testbed and Experiment Engines

7.1 State of the art

7.1.1 Grid'5000

Nearly all the experiments presented in this document have been carried on the Grid'5000 [Bal+13] testbed. Quoting its official website¹: “Grid'5000 is a large-scale and flexible testbed for experiment-driven research in all areas of computer science, with a focus on parallel and distributed computing including Cloud, HPC and Big Data and AI.” It provides dozen of clusters, each one having between 2 and 124 homogeneous compute nodes. There is a high diversity of hardware, including several generations of Intel processors available, AMD and ARM processors, GPU, persistent memory (PMEM) as well as high-performance networks such as Infiniband or Omni-path. Another important feature is the ability for the experimenter to get full control on the nodes, as it is possible to deploy a new operating system and therefore to gain superuser access.

7.1.2 Experiment engines

While it is possible to run a complete experiment on a testbed like Grid'5000 by manually issuing commands in an interactive shell, it is not advisable as it quickly becomes extremely tedious and error-prone. Automating the experiment is a necessary condition to have reproducible results. A first step toward this goal is to write some ad-hoc script. However, two independent experiments might still share a lot of steps that could be refactored in a common layer, e.g. OS deployment, package installation, or even more advanced features like node instrumentation or environment logging.

¹<https://www.grid5000.fr/>

For these reasons, it is a common practice to use an experiment engine. Buchert et al. describe the features of eight different softwares [Buc+15]. To the best of our knowledge, only three offer a native support for Grid'5000, namely Expo, XPFlow and Execo. Unfortunately, Expo and XPFlow are now longer maintained, the last commit in their respective repositories was done on November 2014 and September 2015. For these reasons, the experiment engine Execo [Imb+13] is often recommended to Grid'5000 newcomers.

Experiments with Execo are described as a Python script. We believe this is one of its best qualities, as it offers a lot of freedom and flexibility to the experimenter, comparatively to other experiment engines that use custom domain specific languages (DSL). Yet, we made the choice to not use it. The main reason is that a typical Execo experiment uses a lot of low-level constructs that are really unpleasant and unintuitive to write and read. Section 7.2.2 will present some comparisons. Furthermore, Execo lacks a lot of important features, like node instrumentation and metadata collection, i.e. we would still have needed to implement a lot of functionalities on top of Execo.

7.2 Yet another experiment engine: Peanut

7.2.1 Key features

7.2.2 Comparison with Execo

Randomizing matters!

8.1 Basic effects

Some text...

8.2 Unexpected effects

Some text...

8.3 Beware of extrapolations

Some text...

8.4 Beware of experimental conditions

Some text...

8.5 Conclusion

Some text...

Performance non-regression tests

9.1 State of the art

Some text...

9.2 Performance measure and information collection

Some text...

9.3 Statistical test

Some text...

9.4 Conclusion

DRAFT
4th November 2020, 13:41:54

Conclusion

Your beautiful conclusion. Lorem ipsum dolor sit amet, consectetur adipiscing elit. Ut purus elit, vestibulum ut, placerat ac, adipiscing vitae, felis. Curabitur dictum gravida mauris. Nam arcu libero, nonummy eget, consectetur id, vulputate a, magna. Donec vehicula augue eu neque. Pellentesque habitant morbi tristique senectus et netus et malesuada fames ac turpis egestas. Mauris ut leo. Cras viverra metus rhoncus sem. Nulla et lectus vestibulum urna fringilla ultrices. Phasellus eu tellus sit amet tortor gravida placerat. Integer sapien est, iaculis in, pretium quis, viverra ac, nunc. Praesent eget sem vel leo ultrices bibendum. Aenean faucibus. Morbi dolor nulla, malesuada eu, pulvinar at, mollis ac, nulla. Curabitur auctor semper nulla. Donec varius orci eget risus. Duis nibh mi, congue eu, accumsan eleifend, sagittis quis, diam. Duis eget orci sit amet orci dignissim rutrum.

DRAFT
4th November 2020, 13:41:54

Bibliography

- [@top500] *TOP500 Website*. URL: <https://www.top500.org/> (visited on Sept. 7, 2020).
cit. on p. 1
- [Bad+03] Rosa M. Badia, Jesús Labarta, Judit Giménez, and Francesc Escalé. “Dimemas: Predicting MPI Applications Behaviour in Grid Environments”. In: *Proc. of the Workshop on Grid Applications and Programming Tools*. June 2003. cit. on p. 11
- [Bal+13] Daniel Balouek, Alexandra Carpen-Amarie, Ghislain Charrier, et al. “Adding Virtualization Capabilities to the Grid’5000 Testbed”. In: *Cloud Computing and Services Science*. Ed. by IvanI. Ivanov, Marten Sinderen, Frank Leymann, and Tony Shan. Vol. 367. Communications in Computer and Information Science. Springer International Publishing, 2013. cit. on pp. 15, 33
- [Bir+13] R. F. Bird, S. A. Wright, D. A. Beckingsale, and S. A. Jarvis. “Performance Modelling of Magnetohydrodynamics Codes”. In: *Computer Performance Engineering*. Ed. by Mirco Tribastone and Stephen Gilmore. Berlin, Heidelberg: Springer Berlin Heidelberg, 2013, pp. 197–209. cit. on p. 12
- [Buc+15] Tomasz Buchert, Cristian Ruiz, Lucas Nussbaum, and Olivier Richard. “A survey of general-purpose experiment management tools for distributed systems”. In: *Future Generation Computer Systems* 45 (2015), pp. 1–12. cit. on p. 34
- [Cas+14] Henri Casanova, Arnaud Giersch, Arnaud Legrand, Martin Quinson, and Frédéric Suter. “Versatile, Scalable, and Accurate Simulation of Distributed Applications and Platforms”. In: *Journal of Parallel and Distributed Computing* 74.10 (2014), pp. 2899–2917. cit. on p. 12
- [Cas+15] Henri Casanova, Frédéric Desprez, George S. Markomanolis, and Frédéric Suter. “Simulation of MPI applications with time-independent traces”. In: *Concurrency and Computation: Practice and Experience* 27.5 (Apr. 2015), p. 24. cit. on p. 11
- [CLH19] Tom Cornebize, Arnaud Legrand, and Franz C Heinrich. “Fast and Faithful Performance Prediction of MPI Applications: the HPL Case Study”. In: *2019 IEEE International Conference on Cluster Computing (CLUSTER)*. 2019 IEEE International Conference on Cluster Computing (CLUSTER). Albuquerque, United States, Sept. 2019. cit. on p. 5
- [CLT13] Laura Carrington, Michael Laurenzano, and Ananta Tiwari. “Inferring Large-scale Computation Behavior via Trace Extrapolation”. In: *Proc. of the Workshop on Large-Scale Parallel Processing*. 2013. cit. on p. 12
- [Cor17] Tom Cornebize. “Capacity Planning of Supercomputers: Simulating MPI Applications at Scale”. MA thesis. Grenoble INP ; Université Grenoble - Alpes, June 2017. cit. on p. 5

- [Deg+17] Augustin Degomme, Arnaud Legrand, Georges Markomanolis, et al. “Simulating MPI applications: the SMPI approach”. In: *IEEE Transactions on Parallel and Distributed Systems* 28.8 (Feb. 2017), p. 14. cit. on pp. 12, 13, 19
- [Eng14] Christian Engelmann. “Scaling To A Million Cores And Beyond: Using Light-Weight Simulation to Understand The Challenges Ahead On The Road To Exascale”. In: *FGCS* 30 (Jan. 2014), pp. 59–65. cit. on p. 12
- [Gra+16] Thomas Grass, César Allande, Adrià Armejach, et al. “MUSA: A Multi-level Simulation Approach for Next-generation HPC Machines”. In: *Proceedings of the International Conference for High Performance Computing, Networking, Storage and Analysis*. SC '16. Salt Lake City, Utah: IEEE Press, 2016, 45:1–45:12. cit. on p. 12
- [Gra69] Ronald L. Graham. “Bounds on multiprocessing timing anomalies”. In: *SIAM journal on Applied Mathematics* 17.2 (1969), pp. 416–429. cit. on p. 1
- [Hei+17] Franz C. Heinrich, Tom Cornebize, Augustin Degomme, et al. “Predicting the Energy Consumption of MPI Applications at Scale Using a Single Node”. In: *Proc. of the 19th IEEE Cluster Conference*. 2017. cit. on p. 13
- [Imb+13] Matthieu Imbert, Laurent Pouilloux, Jonathan Rouzaud-Cornabas, Adrien Lebre, and Takahiro Hirofuchi. “Using the EXECO Toolkit to Perform Automatic and Reproducible Cloud Experiments”. In: *2013 IEEE 5th International Conference on Cloud Computing Technology and Science*. IEEE, Dec. 2013. cit. on p. 34
- [Jan+10] Curtis L. Janssen, Helgi Adalsteinsson, Scott Cranford, et al. “A Simulator for Large-scale Parallel Architectures”. In: *International Journal of Parallel and Distributed Systems* 1.2 (2010). <http://dx.doi.org/10.4018/jdst.2010040104>, pp. 57–73. cit. on p. 12
- [LD12] Piotr Luszczek and Jack Dongarra. “Reducing the Time to Tune Parallel Dense Linear Algebra Routines with Partial Execution and Performance Modeling”. In: *Parallel Processing and Applied Mathematics*. Springer Berlin Heidelberg, 2012, pp. 730–739. cit. on p. 11
- [Mub+16] M. Mubarak, C. D. Carothers, Robert B. Ross, and Philip H. Carns. “Enabling Parallel Simulation of Large-Scale HPC Network Systems”. In: *IEEE Transactions on Parallel and Distributed Systems* (2016). cit. on p. 11
- [Pet+16] Antoine Petit, Clint Whaley, Jack Dongarra, Andy Cleary, and Piotr Luszczek. *HPL - A Portable Implementation of the High-Performance Linpack Benchmark for Distributed-Memory Computers*. <http://www.netlib.org/benchmark/hpl>. Version 2.2. Feb. 2016. cit. on p. 7
- [Vel+13] Pedro Velho, Lucas Schnorr, Henri Casanova, and Arnaud Legrand. “On the Validity of Flow-level TCP Network Models for Grid and Cloud Simulations”. In: *ACM Transactions on Modeling and Computer Simulation* 23.4 (Oct. 2013), p. 23. cit. on p. 13
- [WM11] Xing Wu and Frank Mueller. “ScalaExtrap: Trace-Based Communication Extrapolation for SPMD Programs”. In: *Proc. of the 16th ACM Symp. on Principles and Practice of Parallel Programming*. 2011, pp. 113–122. cit. on p. 12

- [ZKK04] Gengbin Zheng, Gunavardhan Kakulapati, and Laxmikant Kale. “BigSim: A Parallel Simulator for Performance Prediction of Extremely Large Parallel Machines”. In: *Proc. of the 18th IPDPS*. 2004. cit. on p. 11

DRAFT

4th November 2020, 13:41:54

List of Figures

1.1. Overview of High Performance Linpack	7
3.1. Replacing the calls to computationally expensive functions by a model allows to emulate HPL at a larger scale.	15
3.2. SMPI shared malloc mechanism: large area of virtual memory are mapped onto the same physical pages.	18
3.3. Panel structure and allocation strategy.	18
3.4. Time complexity and memory consumption are linear in the number of processes but remain mildly quadratic with matrix rank.	20
4.1. Illustrating the realism of modeling for dgemm function	24
4.2. Illustrating the realism of modeling for HPL_dlatcpy function	25
4.3. Illustrating piecewise linearity and temporal variability of high-speed communications on two systems.	26

List of Tables

1.1. Typical runs of HPL	9
------------------------------------	---

Abstract

The English abstract.

Résumé

Le résumé en français.

DRAFT

4th November 2020, 13:41:54